Physicochem. Probl. Miner. Process., 59(6), 2023, 172298

http://www.journalssystem.com/ppmp

Physicochemical Problems of Mineral Processing

ISSN 1643-1049

The effect of microbubbles on coarse particle anionic flotation: analysis and optimization

Ahmed Abbaker [1, 2], Nevzat Aslan [1]

[1] Industrial Engineering Department, Sivas Cumhuriyet University, 58140 Sivas, Türkiye

[2] Department of Mining Engineering, Faculty of Engineering Sciences, Omdurman Islamic University, P.O. BOX Khartoum 10257, Omdurman 382, Sudan

Corresponding author: a7medelmubarak@oiu.edu.sd (Ahmed Abbaker)

Abstract: Since the grinding and chemical reagents required for flotation are expensive, coarse particle flotation reduces grinding costs and makes the subsequent process more accessible and cheaper. Recent studies suggest that the flotation of coarse particles using microbubbles has some advantages. However, a thorough analysis of the effectiveness of various flotation parameters and the impact of their interactions on the recovery of coarse particles in the presence and absence of microbubbles has yet to be fully understood. In the current study, the two-level factorial and Box-Behnken experimental designs were performed to characterize, assess, and optimize the implications of seven numerical (sodium oleate, collector; calcium oxide, activator; MIBC, frother; impeller speed; froth depth; pulp concentration; fine particles) and one categorical (microbubbles) independent parameters on the coarse quartz particles. Characterization revealed that froth depth did not significantly affect the flotation recovery of coarse particles in the mechanical laboratory cell. The effects of the variables in the presence of microbubbles revealed that sodium oleate and impeller speed significantly impacted recovery, followed by calcium oxide and fine particles, both of which had a medium influence, and MIBC and pulp concentration, which had a minimal impact. The recovery of coarse particles increased by 92.714% when microbubbles were used, compared to the estimated maximum recovery under ideal conditions of 62.258% without them. From this, it can be concluded that a high coarse particle flotation recovery is possible by optimizing the hydrodynamic conditions and the chemical environment using microbubbles.

Keywords: coarse particle, microbubbles, anionic collector, optimization, statistical analysis

1. Introduction

The different properties between valuable minerals and gangue have been exploited in each type of separation. Froth flotation takes advantage of differences in the surface properties of minerals, either naturally or induced. The flotation system is a complicated set of variables, as shown in Fig. 1 (Elvers, 1991). This process requires a small size range, depending on the particle's density, which differs from 10 to 150 μm (Duffy et al., n.d.). This relatively narrow size range required costly pulverization and the chemical reagents necessary for the process, making the flotation process one of the most expensive processes in mineral processing (Farrokhpay et al., 2021).

Sub-processes of flotation are the collision of the bubble particles, the attachment (aggregate), and the aggregate stability for transport into the froth phase (Darabi et al., 2019). The high probability of detachment and low attachment efficiency are the leading causes of poor coarse particle flotation recovery (Carlos de F. Gontijo et al., 2007; Darabi et al., 2019; Rahman et al., 2012a; Tao, 2005). It has been suggested that other factors contribute to the low recovery of coarse particles, such as the poor suspension of coarse particles due to their high density, which, in the absence of sufficient turbulence, settle to the bottom of the cell and reduce the likelihood that a particle will be collected (Ata and Jameson, 2013; Duffy et al., n.d.; Jameson, 2010). Furthermore, the high-turbulence environment in the mechanical cell affects the stability of bubble-particle aggregates and increases the probability of

DOI: 10.37190/ppmp/172298

detachment (Ata and Jameson, 2013; Carlos de F. Gontijo et al., 2007; Duffy et al., n.d.; Farrokhpay et al., 2011; Jameson, 2010; Rahman et al., 2012a; Tao, 2005; Xu et al., 2011). The most common flotation machines in the mining industry are mechanically agitated devices. Although most coarse flotation approaches outperform traditional cells, their use in mining and mineral processing is relatively rare due to the high costs and inherent risks of developing and testing new flotation cell designs (Hassanzadeh et al., 2022; Nazari et al., 2022). Moreover, poor recovery, desliming, low flotation rate, low surface energy, and particle detachment are some problems with the current techniques for coarse particle flotation, such as Fluidized-bed flotation cells (Kromah et al., 2022).

Microbubbles, compared to conventional bubbles, attach more readily to particles because of their lower ascending velocity and higher surface. Microbubbles combined with large bubbles cause higher flotation recovery of coarse particles because the bonding between microbubbles and large bubbles is more preferential than the bonding between bubbles and particles, as shown in Fig. 2. In other words, microbubbles act as a secondary collector for particles, reducing a flotation collector dosage, enhancing particle attachment probability, and reducing the detachment probability (Nazari et al., 2019; Nazari and Hassanzadeh, 2020; Tao, 2005). The same method of combining microbubbles with coarse bubbles has been applied successfully for fine and ultrafine particles (Farrokhpay et al., 2020; Rulyov et al., 2018, 2021; Tussupbayev et al., 2016).

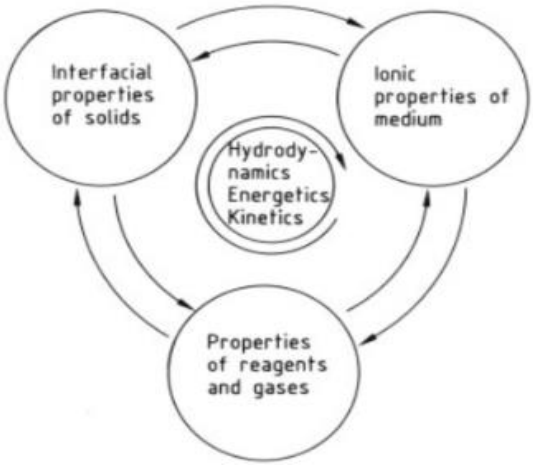

Fig. 1. System variables that affect the flotation process (Elvers, 1991)

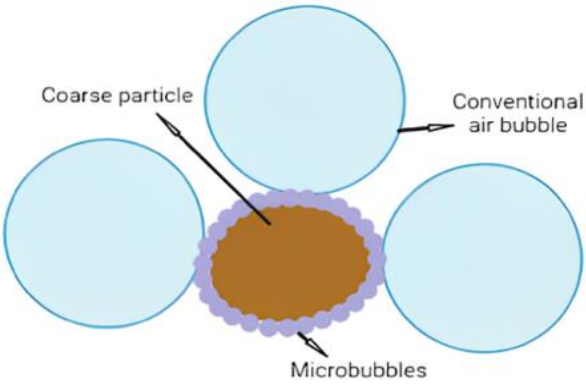

Fig. 2. Contribution of microbubbles to the enhancement of coarse particle flotation

Extending the flotation process's size range will reduce the grinding power consumption and the number of fines produced. Whatever subsequent process gets more accessible and cheaper, such as drying, thickening, and filtration. If the flotation process could be performed at 300 μm rather than 100 μm, the potential energy saving in comminution would be around 30% - 50%. Suppose flotation technology existed, depending on the type of ore. In that case, it might be possible to expand the top grind size to 500μm, float off a significant amount of feed in a primary coarse pass, and then refill the

coarse concentrate to a final size consistent with the release characteristics of the ore (Jameson, 2010; Tao, 2005). Many attempts have been reported to improve a coarse particle's flotation process. However, the lack of testing of some factors and neglect of other important ones resulted in needing more understanding. Compared to those for flotation of finer sizes, the cell hydrodynamic conditions for the flotation of coarse particles are drastically different (Fosu et al., 2015). In addition, the effects of interactions between different variables on the flotation process of coarse particles are not considered. Microbubble-assisted flotation methods are the latest proposed technology and have recently attracted the interest of many scientists. Many conceptual problems remain unsolved regarding their characterization, interface interactions, quantification, influential generations, and the interactive influence of operating parameters. Also, any investigation needs to facilitate the influence of particle-bubble interactions and their modelling in the existence of microbubbles in flotation processes (Nazari and Hassanzadeh, 2020).

This research work aims to fully understand the effect of the flotation parameters of coarse particles (sodium oleate, collector; calcium oxide, activator; MIBC, frother; impeller speed; froth depth; pulp concentration; fine particles) and how microbubbles affect them by using statistical design, analysis, and optimization in a mechanical flotation cell.

2. Materials and methods

2.1. Materials and chemical reagents

A pure quartz sample (≈98%) was received from Kaltun Mining Industry Transport and Fuel Trade in Adyin, Türkiye. The particle size analysis of the representative sample, measured by the Malvern Matersizer, shows that D50 = 276µm, as shown in Fig. 3. As this study focuses on the coarse size, the size of the sample is less than 212µm was removed through a sieve. The particle size measurement was reapplied, resulting in D50 = 495µm, as shown in Fig. 4. Moreover, 10 kg of the sample was pulverized for the use of fine particles in the study, the measurement shows that their size is D50 = 40.2µm. The sample was cleaned using the method of Pashley and Kitchener. The sample was washed three times with concentrated hydrochloride acid (HCl 37%) for two hours each time and then washed with distilled water four times. The sample was then immersed in 30% sodium hydroxide (NaOH) at 60 °C for one minute. Finally, the quartz sample was dried in an oven overnight at 110 °C. After sample preparation, the quartz particles were chemically and mineralogically characterized using X-ray fluorescence (XRF) and X-ray diffraction (XRD) spectrometers, as shown in Table 1 and Fig. 5. Sodium oleate was used as a quartz collector in an anionic state after activation by calcium oxide. Sodium oleate (NaOL, $C_{18}H_{33}NaO_2$) 82% as fatty acids (oleic acid basis) was supplied by SIGMA Life Science, and calcium oxide (CaO) was 97% by Kimylab. The experiments were performed with tap water that had a pH of 7.74.

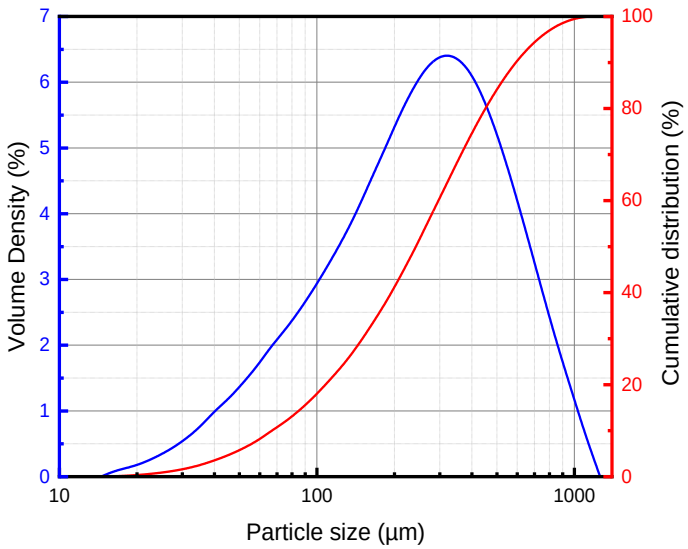

Fig. 3. Size distribution of the sample

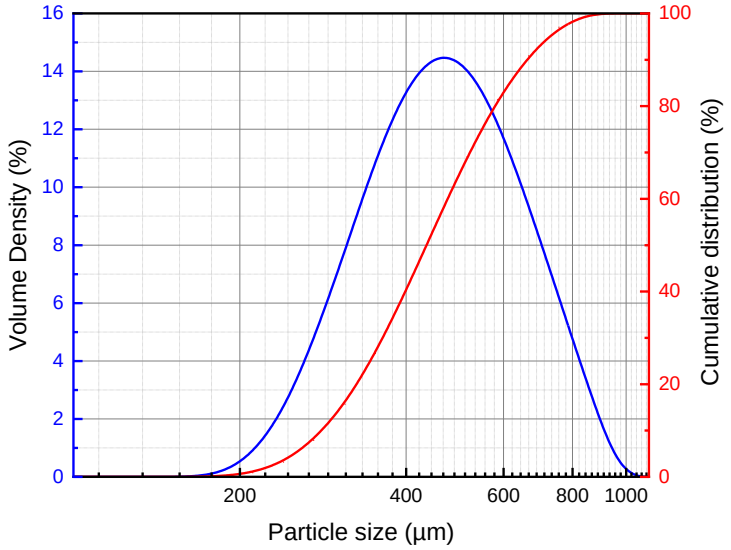

Fig. 4. The size distribution after the removal of 212 µm

Table 1. XRF analysis

Component	SiO_2	Al_2O_3	Na_2O	P_2O_5	TiO_2	MnO	MgO	K_2O	Fe_2O_3	CaO	A.Za
Content (wt.%)	97.7	0.6	0.3	<0.1	<0.1	<0.1	0.1	<0.1	0.4	0.2	0.3

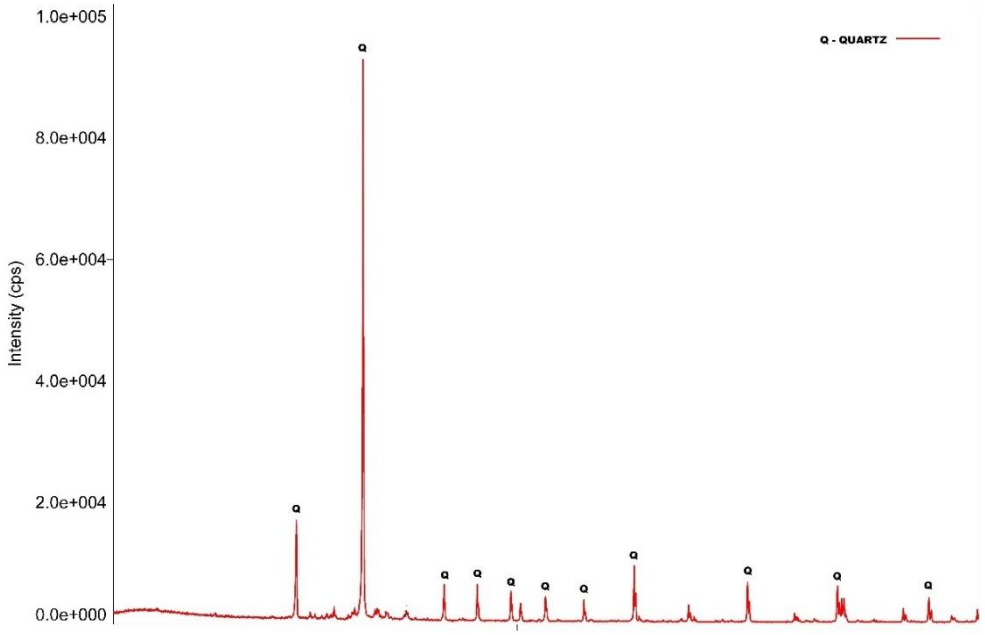

Fig. 5. XRD pattern of quartz

2.1.1. Flotation experiments

A self-aerated Denver flotation machine with size D12 has been used in this study. The flotation time was 4 min in the cell size of 1.2 L at room temperature. For the air flow rate, according to Girgin et al., (2006), an increase of the impeller speed in a self-aerated Denver laboratory equipment resulted in large bubbles. The variables that have a major influence on the outcome will be optimized for any process, and those that have little or no impact on the outcome must be eliminated. By focusing primarily on questionable (uncertain) components, the screening procedure sought to find the factors that have a significant impact on the response. The optimization process then focused on these factors' effects and modelled them.

2.1.2. Screening and characterization

Screening and characterization experiments were conducted to select the significant process parameters from unknown or doubtable parameters under the following conditions: impeller speed 950 rpm, sodium oleate 2.75 mmol/L, pH 12. Flotation experiments (21 runs) were conducted with a two-level factorial design with five centre points to investigate the implication and interactions of MIBC, calcium oxide, pulp concentration, froth depth, and fine particles where their operational ranges have been identified from previous studies as shown in Table 2.

Table 2. Two-level factor design (screening)

Factors	Description	-1	+1
A	MIBC (mmol/L)	0.1	1
B	Calcium oxide (mmol/L)	0.5	5
C	Pulp concentration (%)	10	40
D	Froth depth (cm)	1	3
E	Fine particles D50=40.2 μm (%)	0	20

2.1.3. Optimization

Statistical analysis and optimization of coarse particles were performed utilizing a seven-factor, three-level Box-Behnken experimental design (108 experiments). Six factors are numerical, and one is categorical at pH 12, where Ca^{2+} has the maximum quartz recovery (Maurice and Kenneth, 2003). Table 3 presents the experiments used to optimize the effect and interactions of sodium oleate, MIBC, calcium oxide, impeller speed, pulp concentration, fine particles, and microbubbles.

Table 3. Box-Behnken response surface design (optimization)

Factors	Description	-1	0	+1
A	Sodium oleate (mmol/L)	0.5	2.75	5
B	MIBC (mmol/L)	0.1	0.55	1
C	Calcium oxide (mmol/L)	0.5	2.75	5
D	Impeller speed (rpm)	700	900	1200
E	Pulp concentration (%)	10	25	40
F	Fine particles (%)	0	10	20
G	Microbubbles	Absent		Present

All screening and optimization experiments were randomized to elude bias and eliminate the effects of unexpected variations in the responses. Analysis of variance (ANOVA) was applied to examine the responses to improve the process variables and evaluate their interactions. Five more confirmatory tests were then performed to ensure the best outcome of the statistical experimental design.

2.1.4. Microbubbles generator

Although several technologically viable methods exist for creating micro and nano-bubbles (such as ultrasonic, water-solvent mixture, micro fluids, electrolysis, pressure reduction, and temperature modulation), only some have been designed for flotation systems. It consists of MicroGas (MG), DAF (dissolved air flotation), HC (hydrodynamic cavitation), and CMP (two-phase centrifugal multiphase pump) (Nazari and Hassanzadeh, 2020). Fig. 6 shows a microbubble generator supplied by Dongguan Technology Co. Ltd., China. The pump body of the gas-liquid mixing pump is a direct-connected motor structure. The suction port of the gas-liquid mixing pump uses negative pressure to suck gas, so there is no need to use an air compressor and atmospheric ejector. Due to the pressurized mixing in the pump, the gas and liquid are fully dissolved. Therefore, it is possible to prepare a highly dissolved liquid without a large, pressurized gas tank or expensive reaction tower. The centrifugal pump used

to generate microbubbles has a flow rate of 20 L/min and a gas-liquid ratio of 1:9. The size of microbubbles produced ranges from 20 – 30 µm.

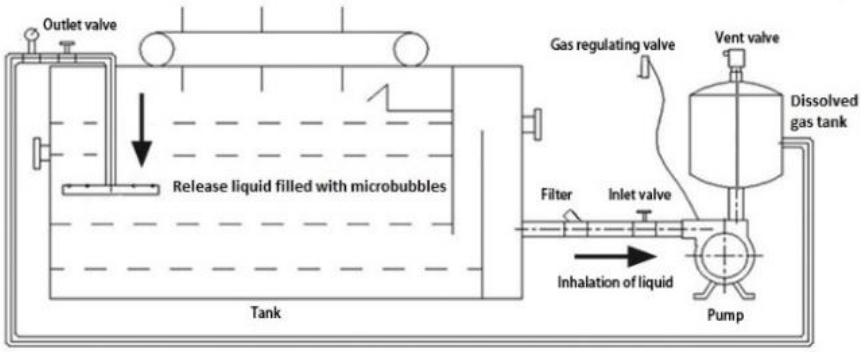

Fig. 5. Microbubbles generator

3. Results and discussion

3.1. Screening and characterization

Calcium oxide (B), followed by fine particles (E) and MIBC (A), had the most considerable impacts, as can be seen from Half-Normal and perturbation plots in Fig. 7. Froth depth (D) and pulp concentration (C) did not directly affect the recovery as they present in perturbation as nearly straight line in Fig. 7(b) and in line in Half-Normal Plot in Fig. 7(a). However, the interaction between fine particles (E) and pulp concentration (C) significantly impacted the response as shown clearly in Fig. 7(a). Because only essential variables and their interactions are needed, froth depth will be eliminated from the optimization process. The role of froth depth is that by decreasing the residence period, a reduction in froth depth promotes the recovery of the coarse particle. On the other hand, when the froth depth was reduced, total recovery slightly rose. However, this would contaminate the concentrate by increasing the recovery of gangue by entrainment (Duffy et al., n.d.; Rahman et al., 2012). Since pure quartz has been used in this study in a 1.2 L flotation cell, its impact on the coarse particle's recovery was marginally small compared to other factors.

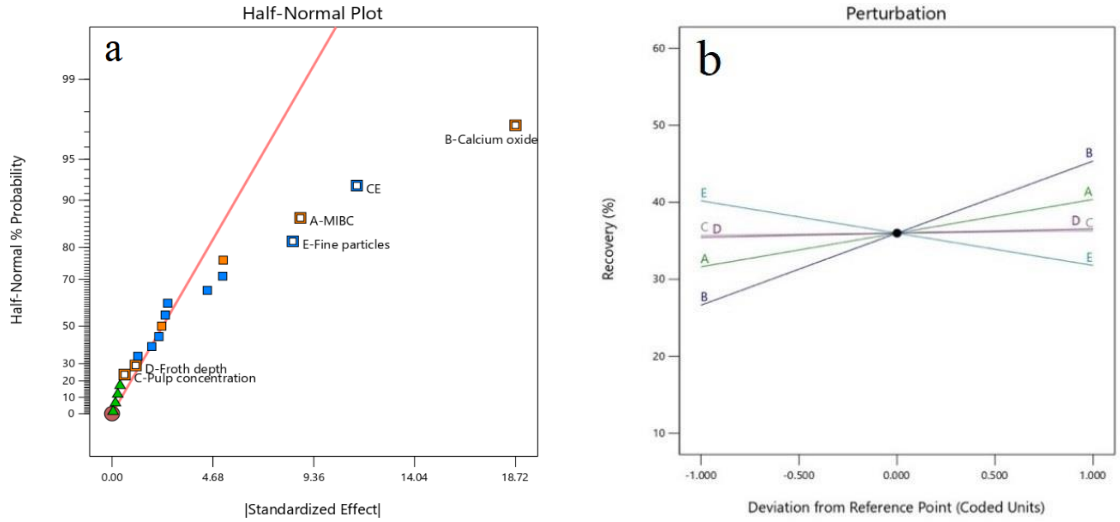

Fig. 6. Shows the main effects of MIBC (A), calcium oxide (B), pulp concentration (C), froth depth (D), and fine particles (E) in (a) Half-Normal and (b) perturbation plots

3.2. Modeling

To illustrate how the experimental models were used to investigate the correlation between process parameters and flotation recovery responses, the following is represented in the quadratic models using a coded factor:

$$\text{Recovery} = 5.11 + 0.9846\,A - 0.043\,B + 0.4961\,C + 0.7802\,D - 0.0425\,E + 0.7126\,F - 0.5595\,G + 0.3868\,AC + 0.1603\,AD + 0.0284\,AE - 0.0566\,AG - 0.2424\,BC + 0.4223\,CD + 0.3196\,CE - 0.1508\,CG - 0.1285\,DG + 0.2614\,EG - 0.8429\,A^2 - 0.3191\,D^2 - 0.2826\,ACG - 0.2381\,ADG + 0.3402\,AEG - 0.2289\,CDG + 0.4607\,D^2G$$

The coded factors equation can be used to predict the response for given levels of each factor. The coefficient's negative sign indicates antagonistic effects, whereas its positive value refers to synergistic effects. More significant factor coefficients imply a factor's particularly substantial influence on flotation performance. The constant value of 5.11 is independent of the operation parameters, where the linear terms of B, E, and G, the quadratic terms of A^2 and D^2, and the interaction terms of AG, BC, CG, ACG, ADG, and CDG have a negative influence on the recovery, indicating that the grade decreases as the value of these terms increases. A, C, D, F, AC, AD, AE, CD, CE, EG, AEG, and D^2G, on the other hand, positively affect the result and show an increase in response as the values of these terminology increase.

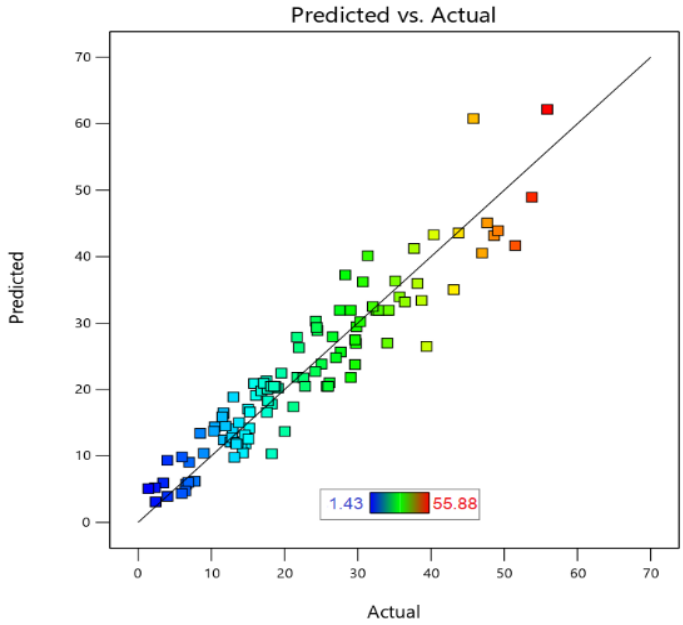

Fig. 7. Correlating predicted values to actual experimental results

The above equation is a good model for predicting flotation recovery, as demonstrated by the statistical lack-of-fit test. The adequate precision measures the signal-to-noise ratio at 25.149. Since this value exceeds 4, it can be used to navigate the design space using the abovementioned model. Additionally, Box-Behnken design data were integrated into the model to assess the validity of the recovery model via the value of the R^2 correlation coefficient. The data collected show that at an R^2 value of 0.8952, the experimental data and the predicted value were highly correlated. The variation in the mean was measured using the adjusted correlation coefficient (adjusted R^2), which was 0.8649. The recovered data closely matched the expected data from the models, as the R^2 and modified R^2 are within 0.20 of one another. The model's standard deviation of 0.5017 is a low value, indicating a good model that produces values almost precisely in line with expected and actual values. Additionally, Fig. 8 presented the association plots between empirical data and predicted recovery responses. The fact that the data was close to a straight line suggests that the response can be predicted using the modelling equations created from the independent elements.

3.3. Perturbation and cubic graphical analysis

Perturbation and cubic plots were used to explain independent variables' main and interaction effects on recovery. The perturbation Fig. 9(a-b) shows the individual primary impacts of sodium oleate (A), MIBC (B), calcium oxide (C), impeller speed (D), pulp concentration (E), and fine particles (F) on the recovery in the absence and presence of microbubbles. As in Fig. 9(a), the variables that have the most

significant impact on recovery in the absence of microbubbles are sodium oleate (A), followed by fine particles (F) and impeller speed (D). In contrast, MIBC (B), pulp concentration (E), and calcium oxide (B) have very little influence. However, Fig. 9(b) illustrates the impact of the variables in the presence of microbubbles, where sodium oleate (A) and impeller speed (D) have significant effects on recovery, followed by calcium oxide (C) and fine particles (F), both of which have a moderate impact, and MIBC (B) and pulp concentration (E) have a negligible impact. The average total recovery has increased by more than 10% since using microbubbles. This outcome may be explained by the increase in the possibility of particle-bubble attachment owing to the existence of microbubbles, thus happened because of the well-known idea of the "bridge effect" or "secondary collector role," where many ultra-fine bubbles on the surface of minerals combine with coarse bubbles (Nazari and Hassanzadeh, 2020).

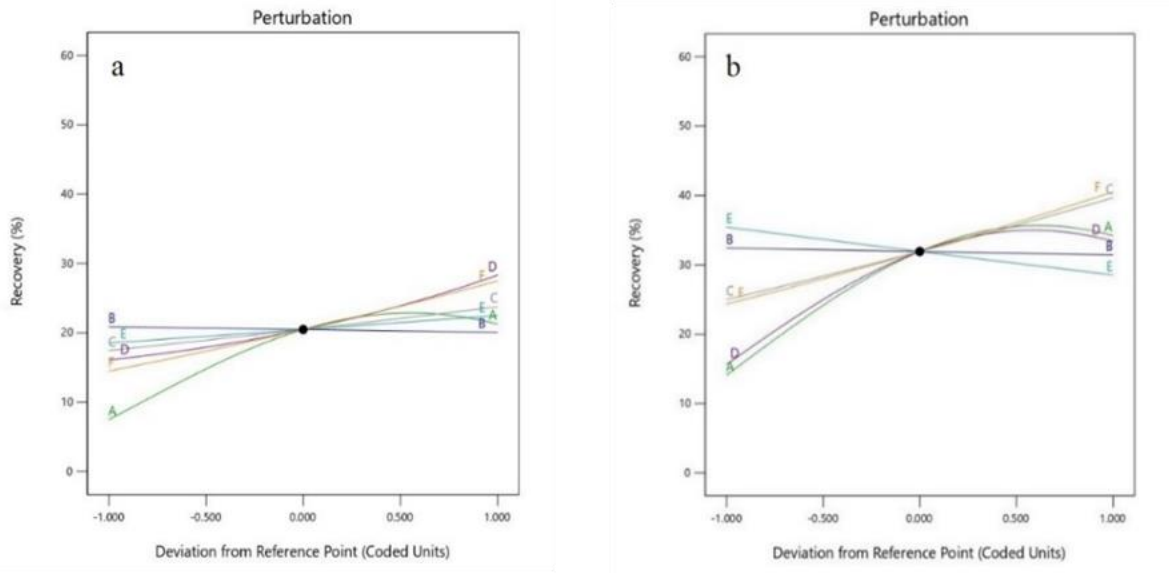

Fig. 8. Perturbation plots of recovery showing the main effects of sodium oleate (A), MIBC (B), calcium oxide (C), impeller speed (D), pulp concentration (E), and fine particles (F); without microbubbles (a) and with microbubbles (b)

Significant interactions exist between calcium oxide, sodium oleate, and other elements. It is well known that the presence of calcium ions, which make quartz positively charged before adding anionic collectors, is required for quartz to float when combined with these collectors (Sobhy et al., 2021). The cubic plots (Fig. 10, 11) illustrate the interaction effects of the MIBC, impeller speed, pulp concentration, and fine particles with sodium oleate and calcium oxide on the recovery value in the absence and presence of microbubbles.

Fig. 10(a) makes it clear that increases in sodium oleate (A) and calcium oxide (C) at all levels had a favourable influence on recovery, except calcium oxide (C) at the high level of MIBC (B), which had very little of an impact on the response. On the other hand, the high level of calcium oxide (C) combined with an increase in MIBC (B) negatively affected the recovery. According to Fig. 11(a), the same effects and interactions of sodium oleate (A), calcium oxide (C), and MIBC (B) almost doubled the recovery values when using microbubbles only for increasing MIBC (B) at the low level of calcium oxide (C) which showed less improvement. (Wiese et al., 2010) suggested that the froth might become unstable and experience poor recovery if the frother is used excessively. Too much frother can produce an overly stable froth that prevents mineral particles from being captured in the concentrate and reports to the tailings. The overall recovery improved in the presence of microbubbles due to their large surface area for the attachment of the hydrophobic particles, increasing the probability of particle-bubble collision and adhesion (Li et al., 2020; Nazari et al., 2019; Tao, 2005).

The response was positively influenced by increasing sodium oleate (A), calcium oxide (C), and impeller speed (D) at all levels of the other two factors, as demonstrated in Fig. 10(b). However, calcium oxide (C) had a slight impact at the low level of both sodium oleate (A) and impeller speed (D). On the other hand, the existence of microbubbles showed a different pattern in Fig. 11(b), where

increasing sodium oleate (A) resulted in a positive impact at all levels except at the low levels of both calcium oxide (C) and impeller speed (D) was not influenced. It is worth mentioning that at high levels of all factors in the presence of microbubbles, the recovery almost doubled compared to their absence. However, other interaction values were almost the same. At slow impeller speed, the probability of collusion decreases as the absence of enough power to mix the heavy particles result in their settling in the pulp and recovery (Nazari et al., 2018). However, the probability of collision and detachment increases at high impeller speed, and the flotation recovery will mostly depend on the attachment between the particle and the bubble (Darabi et al., 2019). Particle-bubble detachment increases with decreasing surface hydrophobicity, resulting in reduced collector coverage (Farrokhpay and Fornasiero, 2017); hence by increasing the amount of collector and activator, the attachment also increases, obtaining high recovery, and by using microbubbles, the recovery becomes even higher. This result explains why the highest recovery values were recorded at the maximum collector, activator, and impeller speed values. This relationship is not infinite since, after a successful collision and attachment, the particle/bubble aggregates generated in the pulp will likely be destroyed under the dominance of severe hydrodynamic circumstances at impeller speeds of more than 1300 rpm (Nazari et al., 2018; Shahbazi et al., 2009).

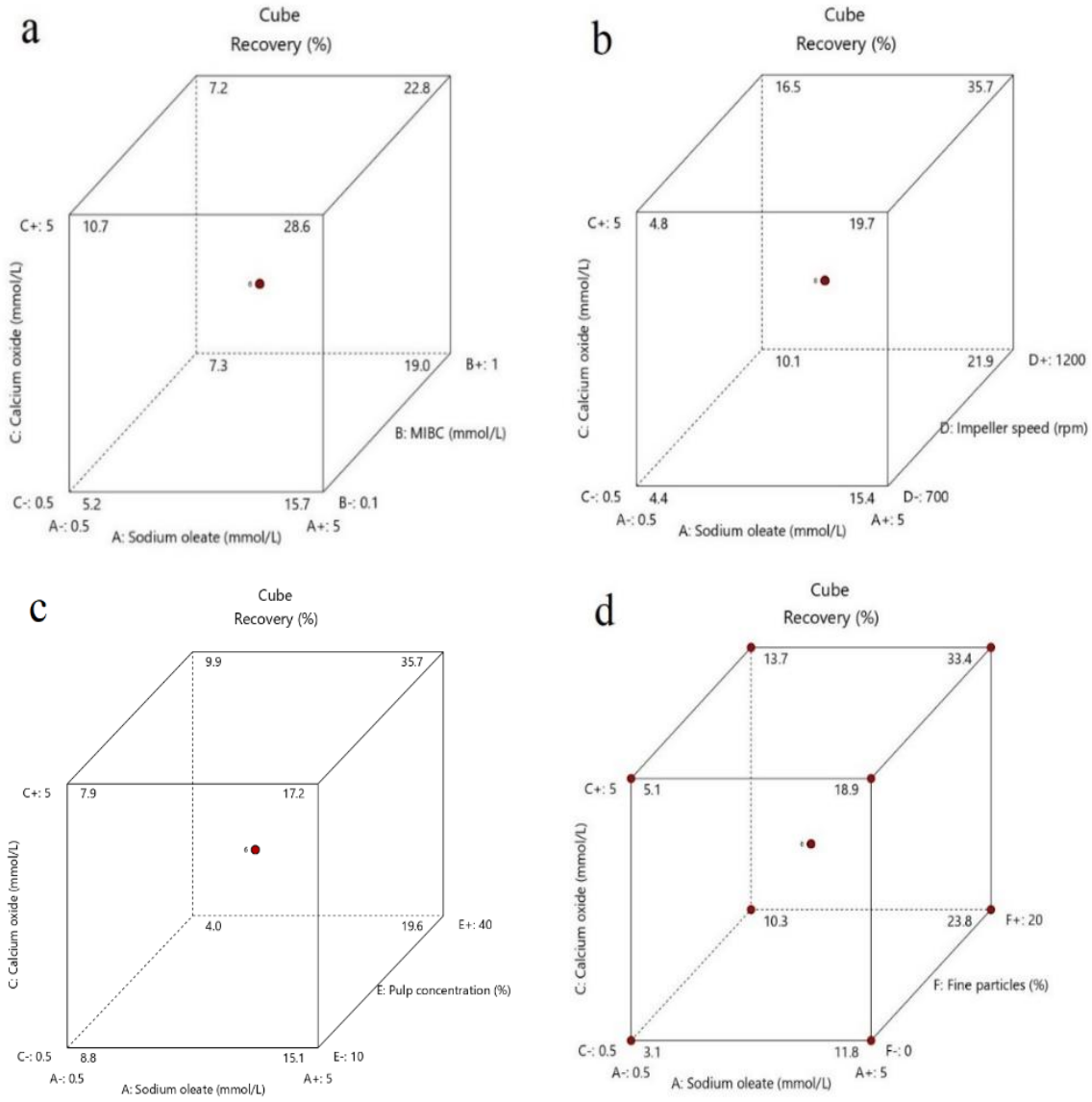

Fig. 9. The cubic graph illustrates how several elements interact to affect the recovery in the absence of microbubbles

Recovery was positively impacted at all levels by increasing sodium oleate (A); The same was valid for calcium oxide (C), except for the low concentrations of both sodium oleate (A) and pulp concentration (E), which were not significantly affected, as shown in Fig. 10(c). Increasing pulp concentration (E) had a positive effect generally. However, it had a detrimental impact when sodium oleate (A) and calcium oxide (C) were at low levels. However, the presence of microbubbles (Fig. 11(c)) showed variable outcomes, where recovery was positively impacted by increasing calcium oxide (C) and sodium oleate (A) at all levels. In addition, the recovery was negatively affected by the increase in pulp concentration s content (E), except for the low sodium oleate content (A) and the high calcium oxide content (C). Without microbubbles, mineral recoveries are often more significant when pulp densities are higher. This outcome happened because a higher pulp density may result in greater particle-bubble collision probabilities, allowing more mineral particles to attach to air bubbles and be transported to the froth phase (Duffy et al., n.d.). Microbubbles improve the flotation pulp's practical volume when they are added to it. They have a higher surface area than more giant bubbles, which raises the pulp's void proportion. As a result, the pulp's bulk density is effectively decreased, lowering the pulp's overall density. Microbubbles may have improved the possibility of particle-bubble attachment and contact angles due to the well-known "bridge effect" or a secondary collector function of microbubbles, in which a large number of ultrafine bubbles on the surface of the minerals bond

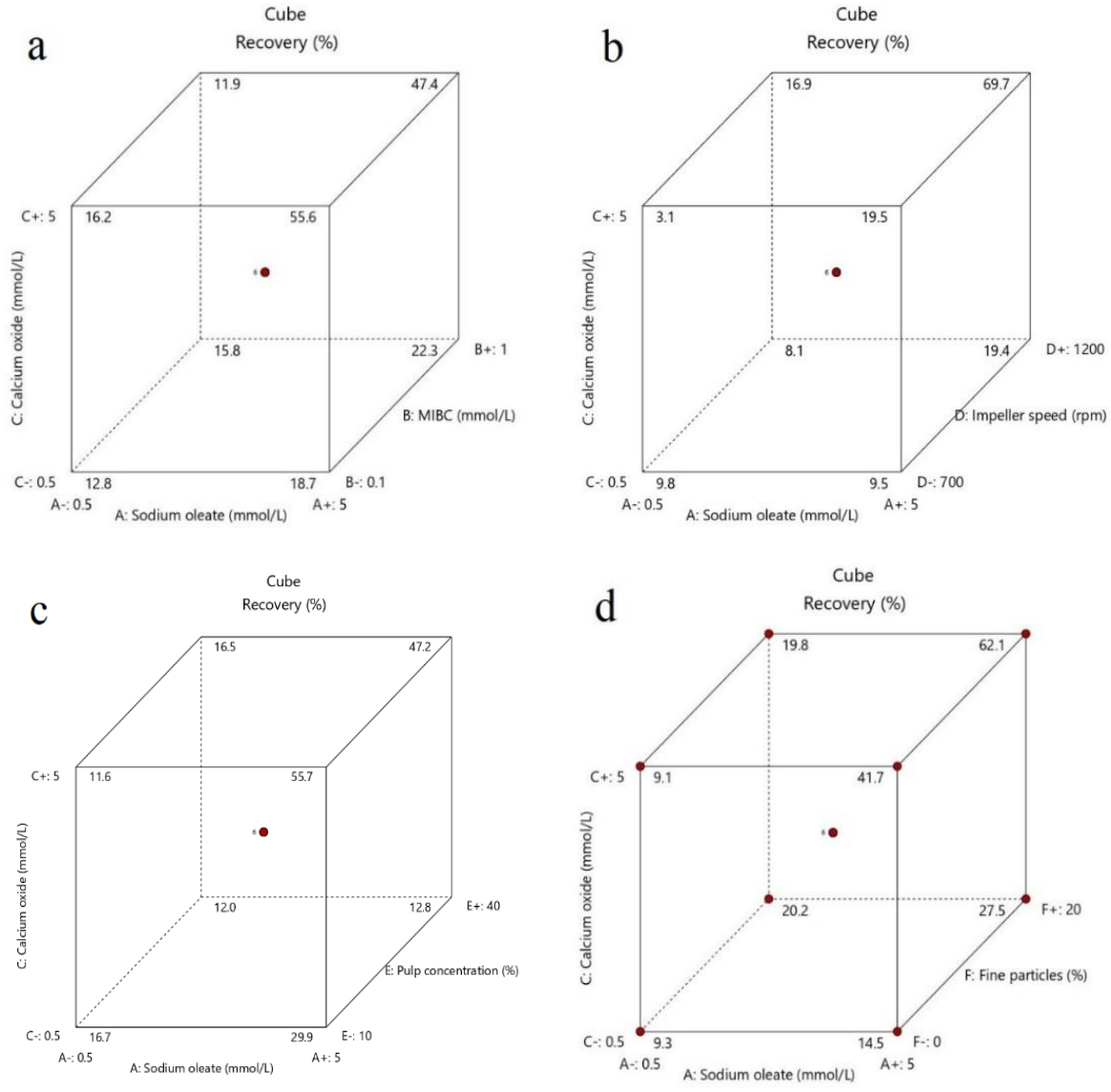

Fig. 10. The cubic graph shows how several elements interact to affect the recovery in the presence of microbubbles

with regular bubbles (Nazari and Hassanzadeh, 2020). At low pulp density, the bridge effect may find a better environment than at high density, which may be the reason for the slight decrease in the recovery in the presence of microbubbles.

According to Fig. 10(d), increasing sodium oleate (A), calcium oxide (C), and fine particles (F) at all levels of the other two parameters showed positive effects on the response in the absence of microbubbles. In Fig. 11(d), increasing calcium oxide (C) had no effect at the low level of sodium oleate (A); otherwise, all factors positively impacted the recovery in the presence of microbubbles. The overall recovery values in the presence of microbubbles were better than in its absence. A certain amount of fine quartz particles in the pulp improved the flotation of coarse quartz, affecting the froth's visual appearance and making the bubbles smaller and more stable, comparable to how frothers work (Ata and Jameson, 2013; Gupta et al., 2007; Vieira and Peres, 2007). The impacts of fine particles in coarse particle flotation might vary depending on several variables, including particle size distribution, particle surface properties, and flotation conditions. The performance of coarse particle flotation may be enhanced, and the detrimental impacts of fine particles can be reduced by optimizing the flotation process parameters.

3.4. The combined effect of parameters

The interactive consequences of each pair of independent factors at the mean value of the other independent factors on the dependent variable of recovery responses were further explained by the 3-D response surface plots.

In the absence and presence of microbubbles, Fig. 12 illustrates the interactive effect of sodium oleate (A) and MIBC (B) at the mean value of calcium oxide (C), impeller speed (D), pulp concentration (E), and fine particles (F). Without microbubbles, the method utilizing intermediate dosages of sodium oleate and MIBC produced the highest recovery of 22%, as shown in Fig. 12(a). In contrast, recovery increased to 36% when microbubbles were used, as presented in Fig. 12(b). Compared to the MIBC factor, sodium oleate in both cases significantly impacted the recovery results. Increasing the amount of sodium oleate (organic surfactant) decreases the surface tension of the pulp according to the Gibbs adsorption equation (Elvers, 1991). It is generally accepted that adding surfactants reduces surface tension, reducing bubble size and creating the same effect as a frother (Cho and Laskowski, 2002). However, the impact of the collector had overcome frother on coarse particle flotation, and the use of microbubbles clarifies this effect. Microbubbles promote even distribution and efficient contact between the bubbles and the hydrophobic particles. Nazari et al., 2019 concluded that in microbubble-assisted flotation, the existence of a collector is capable of compensating for the absence of a frother (Nazari et al., 2019).

In both the absence and presence of microbubbles, the interaction between sodium oleate (A) and calcium oxide (C) is shown in Fig. 13 at the mean value of other parameters. In the case of the absence of microbubbles, calcium oxide had no effect on recovery at sodium oleate concentrations lower than 2.3 mmol/L (Fig. 13(a)); however, as sodium oleate and calcium oxide concentrations were increased, recovery also increased to 26%, demonstrating a proportionate relationship. Fig. 13(b) shows a similar trend. Still, response values were increased twice due to microbubbles, reaching 51% at maximum calcium oxide and sodium oleate levels.

When an anionic collector is present, quartz tends to be poorly buoyant over the entire pH range, but after activation by lime (CaO), its flotability increases dramatically. As shown in Fig. 14(b), calcium species in the solution include hydroxyl calcium ($Ca(OH)^+$), soluble calcium hydroxide ($Ca(OH)_{2(aq)}$, and calcium ions (Ca^{2+}), the concentrations of which depend on the solution's pH (Cao et al., 2022). The dissolution of $Ca(OH)_2$ can be expressed by equations (1), (2), and (3). The pH and concentration affect the types of calcium ions that are present in solutions.

$$Ca(OH)_{2(aq)} \leftrightarrow Ca(OH)^+ + OH^- \quad (1)$$

$$Ca(OH)^+ \leftrightarrow Ca^{2+} + OH^- \quad (2)$$

$$Ca(OH)_{2(aq)} \leftrightarrow Ca^{2+} + 2(OH)^- \quad (3)$$

According to some reports, the species that may adsorb onto the negatively charged surfaces of quartz is $Ca(OH)^+$, which then forms SiO-Ca(OH). By forming covalent bonds, the oleate ions' (Fig. 14

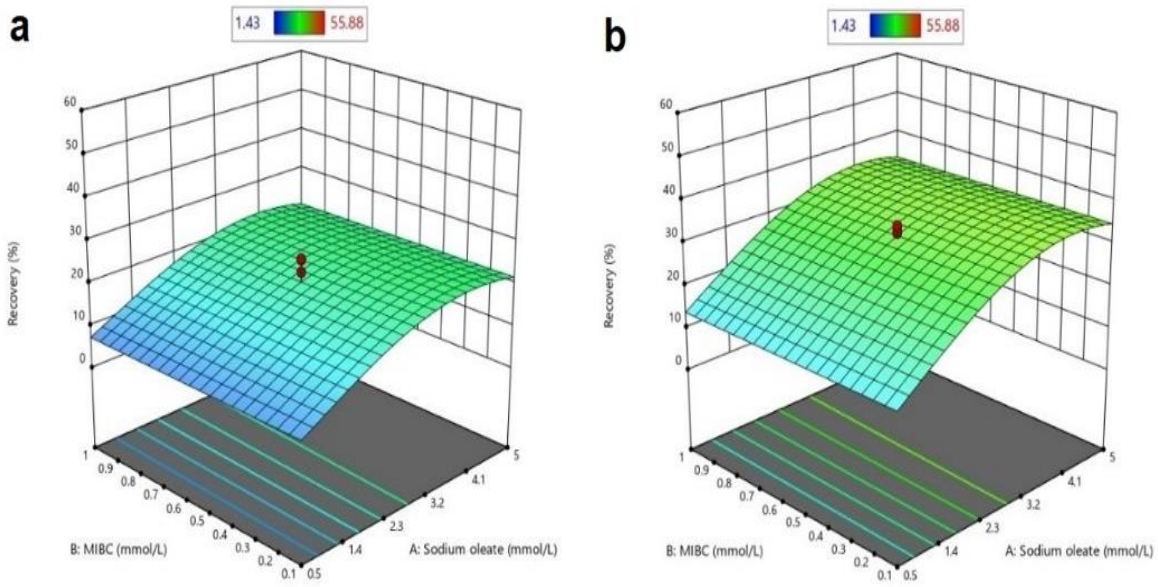

Fig. 12. Response surface presents the interaction between sodium oleate and MIBC affecting the recovery at mean values of other parameters in (a) the absence and (b) the presence of microbubbles

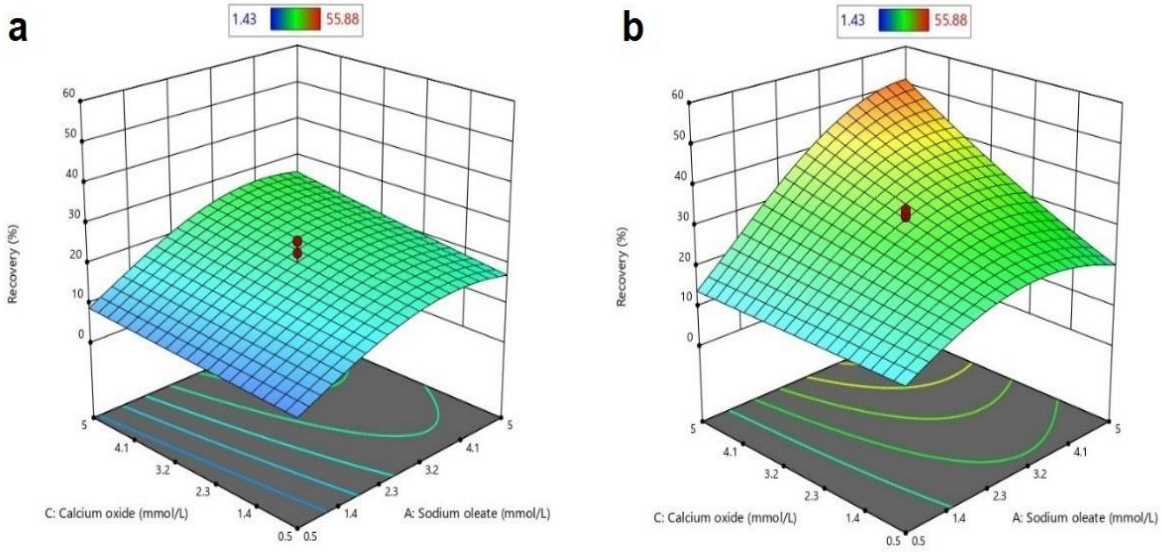

Fig. 13. Response surface shows the interaction between sodium oleate and calcium oxide impacting the recovery at mean values of other parameters in (a) the absence and (b) the presence of microbubbles

(a)) adsorption on the activated quartz surface is referred to as chemisorption. The conventional electron donor/electron acceptor concept, in which the oxygen in the COO^- functional group is the electron donor and the calcium is the electron acceptor, may be used to explain the adsorption. The interactions between the oleate ions and the SiO-Ca(OH) on the quartz surface are shown in equations (4) and (5) (Fan et al., 2020).

$$SiO– Ca(OH) + RCOO^- \rightarrow SiOCaOOCR + OH^- \quad (4)$$

$$2SiO– Ca(OH) + (RCOO)^{-2}{}_2 \rightarrow 2SiOCaOOCR + 2OH^- \quad (5)$$

This phenomenon explains why the adsorption of the collector improved as the amount of activator increased, and microbubbles significantly increased the surface area available for particle-bubble collision, making it easier for hydrophobic particles to adhere to the bubbles.

At the mean levels of MIBC (B), calcium oxide (C), pulp concentration (E), and fine particles (F),

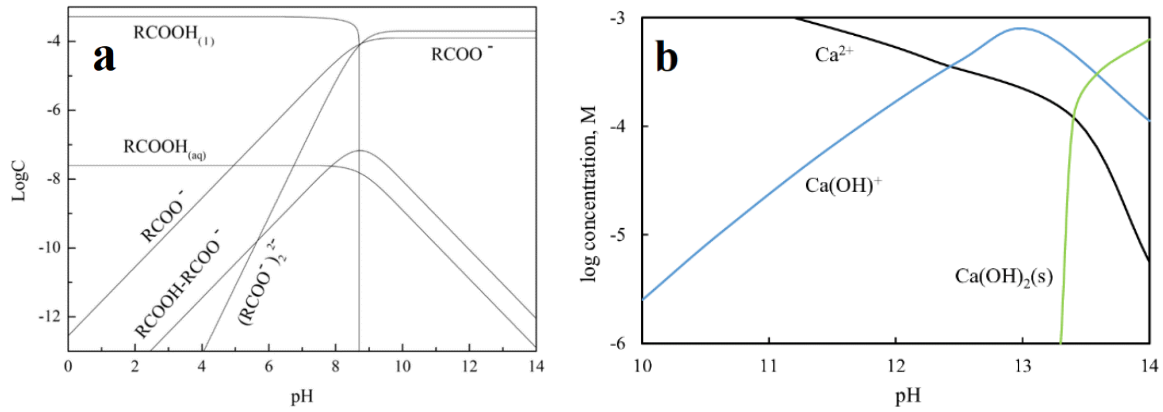

Fig. 14. Species distribution diagram of (a) sodium oleate and (b) calcium oxide as a function of pH

both with and without microbubbles, Fig. 15 illustrates the interaction impact of sodium oleate (A) and impeller speed (D). The recovery reached a maximum of 30% when impeller speed and sodium oleate increased, as shown in Fig. 15(a). As seen in Fig. 15(b), the pattern became more precise than the previous one, and the recovery increased by 10% when microbubbles were used. There is little force to mix the heavy particles, so they settle in the pulp and reduce the probability of collusion. High impeller speed, however, increases the probability of collision, and flotation recovery will largely depend on the connection between particle and bubble.

On the other hand, the aggregates of a particle bubble formed in the pulp are likely to be destroyed under disruptive hydrodynamic conditions. Agitation intensity has an inverse relation effect on the bubble size, where at high speed, the bubbles are smaller than at low speed, and the probability of collision increases (Darabi et al., 2019; Wang and Liu, 2021). The intensity of bubbles from high speed merged with microbubbles enhances the collision and improves the recovery.

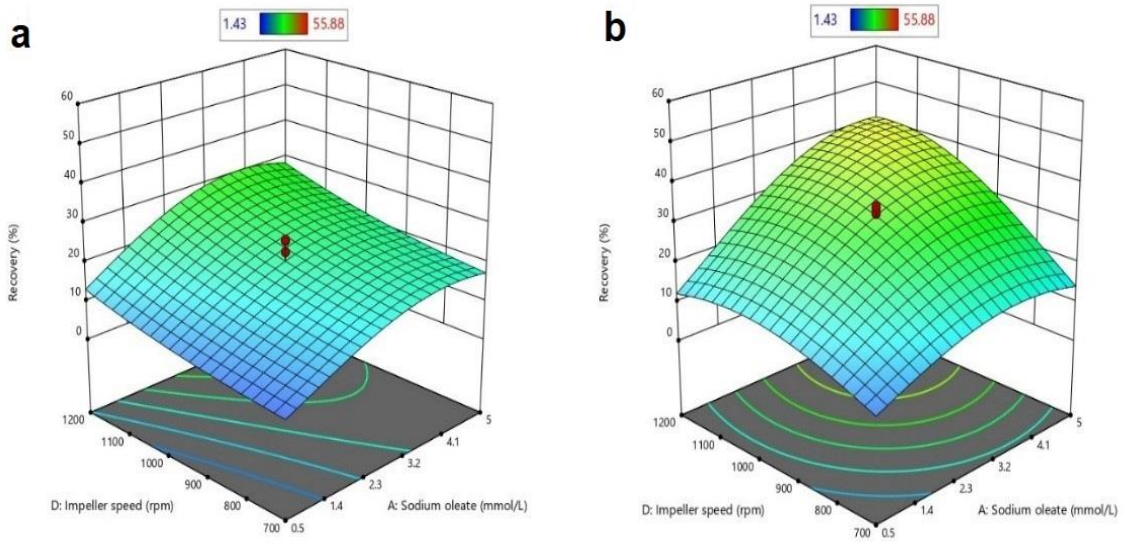

Fig. 15. Response surface displays the interaction between sodium oleate and impeller speed impacting the recovery at mean values of other parameters in (a) the absence and (b) the presence of microbubbles

Fig. 16 illustrates sodium oleate (A) and pulp concentration (E) interaction at mean levels of other variables, with and without microbubbles. In the absence of microbubbles (Fig. 16(a)), pulp concentration had no impact on recovery at sodium oleate concentrations lower than 2.5 mmol/L; nevertheless, recovery improved proportionately to 27% when pulp concentration and sodium oleate were increased. The pulp concentration continued to behave as it had at less than 2.5 mmol/L of sodium oleate in the presence of microbubbles, as shown in Fig. 16(b), but with more remarkable recoveries values. However, when sodium oleate levels rise, and pulp concentration percentages fall,

the response rises to 40%. As discussed earlier, higher pulp densities frequently result in increased mineral recoveries. A higher pulp density may increase the likelihood that mineral particles collide with air bubbles and go to the froth phase. The addition of microbubbles increases the flotation pulp's adequate volume. They have a larger surface area than larger bubbles, increasing the pulp's void fraction. The pulp's total density is subsequently reduced due to the reduction in bulk density.

The interaction between sodium oleate (A) and fine particles (F) is presented in Fig. 17 at the mean value of other parameters in both the existence and absence of microbubbles. At sodium oleate concentrations less than 1.5 mmol/L, fine particles had no impact on recovery in the absence of microbubbles (Fig. 17(a)); however, when sodium oleate and fine particles concentrations increased, recovery also climbed to 30%, suggesting a proportional connection. Similar trends may be seen in Fig. 17(b); nevertheless, the microbubbles enhanced response values, which exceeded 44% at the highest levels of sodium oleate and fine particles. The existence of fine particles makes the bubbles smaller and more stable and thus increasing coarse particle recovery. Particles significantly impact froth stability by preventing bubbles from coalescing and retaining greater bubble surface area throughout the froth zone. Due to their increased bulk, coarse particles are thought to break thin films, causing froth collapse and instability quickly.

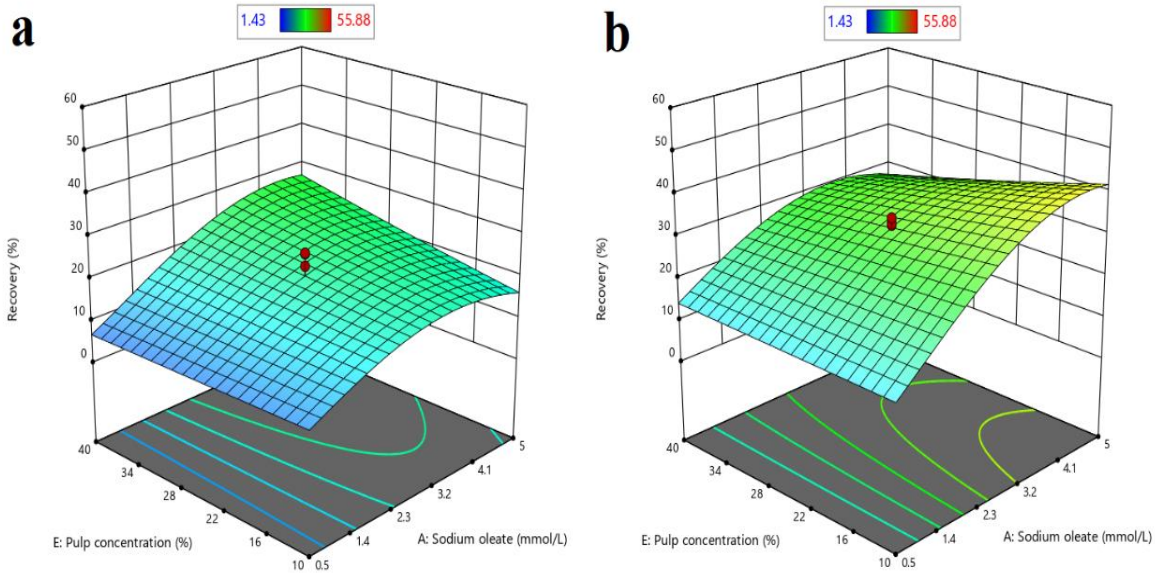

Fig. 16. Response surface presents the interaction between sodium oleate and pulp concentration impacting the recovery at mean values of other parameters in (a) the absence and (b) the presence of microbubbles

Fine particles may have served as binding agents in bubble clusters. They can better carry the associated coarse particles at the interface because of their enhanced buoyancy in a secure transportation structure. It is not immediately evident why the rate at which coarse particles are collected has increased in the presence of fines. One theory is that by limiting surface mobility or the three-phase contact line on the particle surface, the presence of small particles on the surfaces of bubbles may stabilize the air-liquid interface. Additionally, reducing bubble surface deformation creates a more secure environment for the coarse particles to be transported without the risk of being dislodged as the bubble rises in the liquid (Rahman et al., 2012).

3.5. Optimization

Setting the required response objectives helps the experimental design optimize process conditions. The current investigation aimed to optimize and maximize coarse particle flotation recovery. According to the 3-D response surface plots, the ideal flotation conditions were found to be 4.366 mmol/L sodium oleate, 0.133 mmol/L MIBC, 4.997 mmol/L calcium oxide, 1199.796 rpm impeller speed, 39.968% pulp concentration, and 19.922% fine particles in the absence of microbubbles, which led to the highest recovery of 62.258%. On the other hand, optimal flotation conditions in the presence

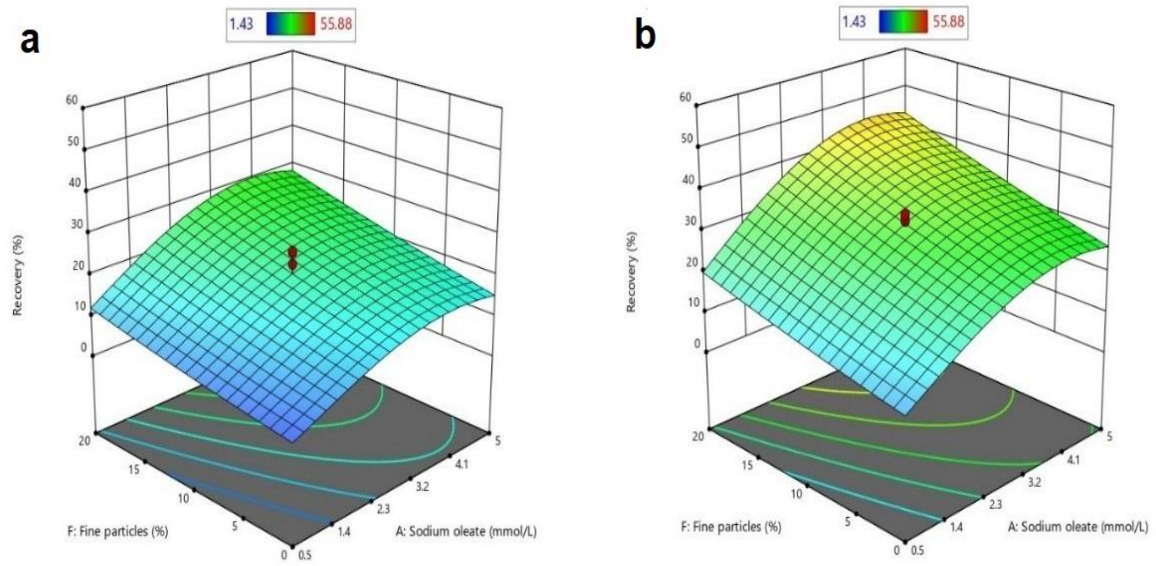

Fig. 17. Response surface shows the interaction between sodium oleate and fine particles impacting the recovery at mean values of other parameters in (a) the absence and (b) the presence of microbubbles

of microbubbles were determined to be 5 mmol/L sodium oleate, 0.101 mmol/L MIBC, 4.997 mmol/L calcium oxide, 1199.974 rpm impeller speed, 10.736% pulp concentration, and 20% fine particles, which resulted in a maximum recovery of 92.714%. Five verification flotation experiments were carried out for each categorical level of microbubbles under optimal conditions after the ideal flotation conditions had been developed to assess the outcomes of the Box-Behnken design and optimization. The average recovery from these verification tests was within the expected range and agreed well with the projected values, indicating that the proposed model can improve flotation performance.

4. Conclusions

Reduced costs for grinding, filtration, thickening, drying, and increased plant throughput are just a few benefits of coarse particle flotation. In this study, anionic flotation experiments were statistically designed using a two-factorial level (for screening and characterization) and Box-Behnken methods performed in a mechanical flotation cell. The characterization result showed that froth depth had no significant effects on the recovery of coarse particle flotation in the mechanical laboratory cell. The impact of the variables in the presence of microbubbles showed that sodium oleate (A) and impeller speed (D) had a significant effect on recovery, followed by calcium oxide (C) and fine particles (F), both of which had a moderate impact, and MIBC (B) and pulp concentration (E) had a negligible impact. The predicted maximum recovery at optimum conditions without microbubbles was 62.258%; conversely, by using microbubbles, the recovery of coarse particles reached 92.714%. Future investigations are required concerning the behaviour of microbubbles in different chemical environments and how they relate to hydrodynamic conditions.

References

ATA, S., JAMESON, G.J., 2013. *Recovery of coarse particles in the froth phase–A case study*. Miner. Eng., 45, 121–127.

CAO, S., YIN, W., YANG, B., ZHU, Z., SUN, H., SHENG, Q., CHEN, K., 2022. *Insights into the influence of temperature on the adsorption behavior of sodium oleate and its response to flotation of quartz*. Int. J. Min. Sci. Technol., 32, 399–409.

CARLOS DE F. GONTIJO, D. FORNASIERO, J. RALSTON, 2007. *The limits of fine and coarse particle flotation*. Canad. J. Chem. Eng., 85(5), 739-747.

CHO, Y.S., LASKOWSKI, J.S., 2002. *Effect of flotation frothers on bubble size and foam stability*, Int. J. Miner. Process., 64, 69-80.

DARABI, H., KOLEINI, S.M.J., DEGLON, D., REZAI, B., ABDOLLAHY, M., 2019. *Investigation of bubble-particle interactions in a mechanical flotation cell, part 1: Collision frequencies and efficiencies*. Miner. Eng., 134, 54–64.

DUFFY, K.-A., RUNGE, K., TABOSA, E., N.D. 2013. *Strategies for increasing coarse particle flotation in conventional flotation cells*, Proceedings Flotation, Cape Town, South Africa.

ELVERS, B., 1991. *Ullmann's encyclopedia of industrial chemistry*. Verlag Chemie Hoboken, NJ.

FAN, G., WANG, L., CAO, Y., LI, C., 2020. *Collecting agent–mineral interactions in the reverse flotation of iron ore: A brief review*. Minerals, 10, 681.

FARROKHPAY, S., AMETOV, I., GRANO, S., 2011. *Improving the recovery of low grade coarse composite particles in porphyry copper ores*, Advanced Powder Technology., 22, 464–470.

FARROKHPAY, S., FILIPPOV, L., FORNASIERO, D., 2021. *Flotation of fine particles: A review*. Mineral Processing and Extractive Metallurgy Review, 42, 473–483.

FARROKHPAY, S., FILIPPOVA, I., FILIPPOV, L., PICARRA, A., RULYOV, N., FORNASIERO, D., 2020. *Flotation of fine particles in the presence of combined microbubbles and conventional bubble*s. Miner. Eng., 155, 106439.

FARROKHPAY, S., FORNASIERO, D., 2017. Flotation of coarse composite particles: *Effect of mineral liberation and phase distribution*. Advanced Powder Technology, 28, 1849–1854.

FOSU, S., AWATEY, B., SKINNER, W., ZANIN, M., 2015. *Flotation of coarse composite particles in mechanical cell vs. the fluidised-bed separator (The HydroFloat™)*. Miner. Eng., 77, 137–149.

GIRGIN, E.H., DO, S., GOMEZ, C.O., FINCH, J.A., 2006. *Bubble size as a function of impeller speed in a self-aeration laboratory flotation cell*. Miner. Eng., 19, 201–203.

GUPTA, A.K., BANERJEE, P.K., MISHRA, A., 2007. *Effect of frothers on foamability, foam stability, and bubble size*. Coal Preparation, 27, 107–125.

HASSANZADEH, A., SAFARI, M., HOANG, D.H., KHOSHDAST, H., ALBIJANIC, B., KOWALCZUK, P.B., 2022. *Technological assessments on recent developments in fine and coarse particle flotation systems*. Miner. Eng., 180, 107509.

JAMESON, G.J., 2010. *Advances in fine and coarse particle flotation, in: Canadian Metallurgical Quarterly*. Maney Publishing, 328–330.

KROMAH, V., POWOE, S.B., KHOSRAVI, R., NEISIANI, A.A., CHELGANI, S.C., 2022. *Coarse particle separation by fluidized-bed flotation: A comprehensive review*. Powder Technol., 409, 117831.

LI, Y., WU, F., XIA, W., MAO, Y., PENG, Y., XIE, G., 2020. *The bridging action of microbubbles in particle-bubble adhesion*. Powder Technol., 375, 271–274.

MAURICE, C.F., KENNETH, N., 2003. *Principle of Mineral Processing*. Society of Mining, Metallurgy, and Exploration. Inc.(SME), Georgia, 245–299.

NAZARI, S., CHEHREH CHELGANI, S., SHAFAEI, S.Z., SHAHBAZI, B., MATIN, S.S., GHARABAGHI, M., 2019. *Flotation of coarse particles by hydrodynamic cavitation generated in the presence of conventional reagents.* Sep. Purif. Technol., 220, 61–68.

NAZARI, S., HASSANZADEH, A., 2020. *The effect of reagent type on generating bulk sub-micron (nano) bubbles and flotation kinetics of coarse-sized quartz particles*. Powder Technol., 374, 160–171.

NAZARI, S., HASSANZADEH, A., HE, Y., KHOSHDAST, H., KOWALCZUK, P.B., 2022. *Recent Developments in Generation, Detection and Application of Nanobubbles in Flotation.* Minerals. 12(4), 462.

NAZARI, S., SHAFAEI, S.Z., GHARABAGHI, M., AHMADI, R., SHAHBAZI, B., 2018. *Effect of frother type and operational parameters on nano bubble flotation of quartz coarse particles.* Journal of Mining & Environment, 9, 539–546.

RAHMAN, R.M., ATA, S., JAMESON, G.J., 2012. *The effect of flotation variables on the recovery of different particle size fractions in the froth and the pulp.* Int. J. Miner. Process., 106–109, 70–77.

RULYOV, N., NESSIPBAY, T., DULATBEK, T., LARISSA, S., ZHAMIKHAN, K., 2018. *Effect of microbubbles as flotation carriers on fine sulphide ore beneficiation.* Mineral Processing and Extractive Metallurgy, 127, 133–139.

RULYOV, N.N., SADOVSKIY, D.Y., RULYOVA, N.A., FILIPPOV, L.O., 2021. *Column flotation of fine glass beads enhanced by their prior heteroaggregation with microbubbles.* Colloids Surf. A.: Physicochem. Eng. Asp., 617, 126398.

SHAHBAZI, B., REZAI, B., KOLEINI, S.M.J., 2009. *The effect of hydrodynamic parameters on probability of bubble–particle collision and attachment*. Miner. Eng., 22, 57–63.

SOBHY, A., WU, Z., TAO, D., 2021. *Statistical analysis and optimization of reverse anionic hematite flotation integrated with nanobubbles.* Miner. Eng., 163, 106799 .

TAO, D., 2005. *Role of Bubble Size in Flotation of Coarse and Fine Particles - A Review*. Sep Sci Technol. 39, 741-760.

TUSSUPBAYEV, N.K., RULYOV, N.N., KRAVTCHENCO, O. V, 2016. *Microbubble augmented flotation of ultrafine chalcopyrite from quartz mixtures.* Mineral Processing and Extractive Metallurgy, 125, 5–9.

VIEIRA, A.M., PERES, A.E.C., 2007. *The effect of amine type, pH, and size range in the flotation of quartz*. Miner. Eng., 20, 1008–1013.

WANG, D., LIU, Q., 2021. *Hydrodynamics of froth flotation and its effects on fine and ultrafine mineral particle flotation: A literature review*. Miner. Eng., 173, 107220.

WIESE, J.G., HARRIS, P.J., BRADSHAW, D.J., 2010. *The effect of increased frother dosage on froth stability at high depressant dosages,* Miner. Eng., 23, 1010–1017.

XU, D., AMETOV, I., GRANO, S.R., 2011. *Detachment of coarse particles from oscillating bubbles – The effect of particle contact angle, shape and medium viscosity*. Int. J. Miner. Process., 101, 50–57.